

Spin-thermodynamics of cold spin-1 atoms decoupled from spatial modes

Z. B. Li, D. X. Yao, and C. G. Bao*

We study the thermodynamic properties of cold spin-1 atoms with a fixed magnetization M and decoupled from spatial modes. Three temperature domains are found: $(0, T_1)$ is a domain of second condensation, namely, both the spatial and spin degrees of freedom are frozen; (T_1, T_2) is a T -sensitive domain, where the internal energy $U \propto T$, entropy $S_E \propto \log T$, and $U/k_B T$ is always less than $3/2$; (T_2, T_3) is the third domain with a maximum entropy. When T is higher than T_3 , the spatial modes can not be neglected. The appearance of these domains originates from the two gaps: (i) The gap between the ground state and the first excited state, and (ii) the gap between the highest spin-state without spatial excitation and the lowest state with a spatial mode excited. These two gaps are crucial to the low temperature physics and they can be tuned.

PACS numbers: 03.75.Hh, 03.75.Mn, 03.75.Nt

Since the pioneering experiment on spinor condensation [1], the study of these artificial and tunable systems becomes a hot topic [1–8]. Due to the rapid development of low-temperature techniques [9–12], a magnificent goal is to explore the domain below the spatial condensation temperature T_c . In this domain, the condensation can be regarded as a pure spin-system with the frozen spatial modes. Furthermore, when the particle number N is fixed and the magnetization M is conserved, the dimension of the spin-space is given by $(N - M + 2)/2$. Thus the dimension is tunable and could be very low. In addition to the theoretical interest, the low dimensional spin-systems are very promising for important applications. For example, a two-dimensional system could be used as a quantum bit [13, 14]. Furthermore, a recent paper shows that the spin oscillation of a highly multi-spatial-mode thermodynamical gas can be described by a theory without considering the spatial degrees of freedom [15]. It implies that, the spin-mode can be decoupled from the spatial mode under certain conditions. Therefore, the study of a pure spin-system is meaningful. The purpose of this paper is to (i) explore the thermodynamic properties [16] of a pure spin-system and the way to measure them, and (ii) find out the conditions that a condensate can be considered as a pure spin-system.

Consider N spin-1 bosons trapped by an isotropic harmonic potential (HP) $\frac{1}{2}m\omega^2 r^2$. Firstly, the magnetic field B is assumed to be zero. Then, the effect of a residual B is studied. When the dipole-dipole interaction is negligible and $B = 0$, both the total spin S and M are conserved. When the spatial excitation is not involved, the eigenstates can be written as $\Psi_{SM} = \Pi_i \phi_S(\mathbf{r}_i) \vartheta_{SM}^N$, where $\phi_S(\mathbf{r}_i)$ can be obtained by solving the generalized Gross-Pitaevskii equation conserving both S and M [17], ϑ_{SM}^N is the normalized all-symmetric spin-state with good quantum numbers S and M . This spin-state is unique for a pair of (S, M) , and $N - S$ must be even due to the boson statistics [17, 18]. The eigenenergy relative to the ground state (g.s.) is

$$E_S = \frac{c_S}{2} [S(S+1) - S_g(S_g+1)], \quad (1)$$

where $c_S = c_2 \int |\phi_S(\mathbf{r})|^4 d\mathbf{r}$, c_2 is the strength of the spin-dependent interaction. It was found that $|(c_S - c_{S'})/c_S| < 0.02$ in relevant cases. Therefore the subscripts in c_S and ϕ_S can be dropped. S_g is the total spin of the g.s., we have $S_g = N$ (if $c_2 < 0$, say, ^{87}Rb) or $= M'$ (if $c_2 > 0$, say, ^{23}Na), where $M' = M$ (or $M+1$) if $N - M$ is even (or odd), and $M \geq 0$ is assumed.

When the system approaches the thermodynamic equilibrium, it can be treated as a canonical ensemble. The partition function is $Z(c, T) \equiv \sum'_S e^{-\beta E_S}$, where S is from M' to N with even $N - S$, and $\beta = 1/k_B T$. The internal energy $U(c, T) = -\frac{\partial}{\partial \beta} \ln Z$, the specific heat $C(c, T) = \frac{\partial U}{\partial T}$, and the entropy $S_E(c, T) = k_B \ln Z + U/T$. Since c is adjustable, the specific strength $Y(c, T) \equiv \frac{\partial U}{\partial c}$ is further defined to connect other state functions.

One can prove that U satisfies the partial differential equation as

$$\left(T \frac{\partial}{\partial T} + c \frac{\partial}{\partial c} - 1\right) U(c, T) = 0. \quad (2)$$

The other three functions satisfy

$$T \frac{\partial F}{\partial T} + c \frac{\partial F}{\partial c} = 0, \quad (3)$$

where F represents C , Y , or S_E . They are subjected to the boundary conditions listed in Table I. When $T \rightarrow \infty$ or $c \rightarrow 0$, all the weights $e^{-\beta E_S} \rightarrow 1$. Thus, $Z \rightarrow N_{state}$, where $N_{state} = (N - M' + 2)/2$ is the dimension of the spin-space. In the same limit, $U \rightarrow |cN_U|$, $N_U = -(N - M')(4N + 2M' + 1)/12$ (if $c < 0$) or $(N - M')(2N + 4M' + 5)/12$ (if $c > 0$), which is proportional to the direct sum of the eigenenergies, and U/T will tend to zero. Therefore, the entropy $S_E/k_B \rightarrow \ln Z = \ln N_{state}$ as shown in Table I. Whereas when $T \rightarrow 0$ or $|c| \rightarrow \infty$, the weight of the g.s. is one while all the other weights become zero. Since the g.s. is not degenerate, S_E vanishes in this limit.

Additionally, U satisfies $T^2 \frac{\partial^2 U}{\partial T^2} - c^2 \frac{\partial^2 U}{\partial c^2} = 0$. From this equation, we obtain a relation between C and Y as $T \frac{\partial C}{\partial T} = -c \frac{\partial Y}{\partial T}$ and $T \frac{\partial C}{\partial c} = -c \frac{\partial Y}{\partial c}$. They imply that C and Y can vary simultaneously with T and/or c if $c < 0$,

or they vary oppositely if $c > 0$. Moreover, we have $\frac{\partial S_E}{\partial T} = C/T$ and $\frac{\partial S_E}{\partial c} = -C/c$. Thus the increasing of T always leads to an increase of S_E , while the increasing of $|c|$ always leads to a decrease of S_E . In particular, Eq. (2) relates the three thermodynamic functions to each other, $U = TC + cY$.

Numerical examples are shown in Fig. 1, where the realistic parameters of interaction are used. The variation of thermodynamic functions versus T shows three steps: insensitive, sensitive, and insensitive again. For example, the U of Rb and Na remains to be zero when T is very low. Once T is higher than a turning point T_1 , a sudden increasing of U happens (as shown in Fig.1a). When T is higher than the second turning point T_2 , U does not increase any more and remains $\approx |cN_U|$. Note that the energy gap between the g.s. and the first excited state is $E_{gap,1} = |c|(2N - 1)$ (if $c < 0$) or $= |c|(2M' + 3)$ (if $c > 0$). Thus, when M' is small, the gap for Rb is much larger than the gap for Na. On the other hand, we find T_1 for Rb is much larger than the one for Na from Figs. 1a and 1e. Therefore, a larger gap might lead to a higher T_1 . Furthermore, for Na, among the three curves in Fig. 1e with different M , the dotted curve with $M = 1500$ has the largest T_1 . It suggests also that a larger gap might give a higher T_1 .

The domain (T_1, T_2) is a T -sensitive domain, where U increases almost linearly with T (accordingly C is close to a constant), and also S_E increases nearly linearly with $\ln T$ disregarding $c < 0$ or $c > 0$. When $c < 0$, we know from Fig. 1b and 1c that the variations of C and Y are synchronous as predicted. Whereas they behave Oppositely when $c > 0$ as shown in Figs. 1f and 1g. It is worth to point out that the lower part of the spectrum depends (does not depend) on M if $c > 0$ (< 0). Therefore, all the curves in Fig. 1 for Na depend on M strongly, while those for Rb do not.

In the g.s., both the spatial and spin degrees of freedom are frozen. This can be called the second condensation [12]. The probabilities at the g.s. is $P_g = 1/Z$. When $T = 0$, $P_g = 1$. When P_g decreases from 1, the spin-fluctuation begins. The probability at the highest spin-state is $P_{top} = e^{-\beta E_{top}} / Z$, where $E_{top} = \frac{|c|}{2}[N(N+1) - M'(M'+1)]$ is the energy difference between the highest and the lowest spin-states. Note that, in the pure spin-space, $\lim_{T \rightarrow \infty} P_{top} \rightarrow 1/N_{state}$. Thus

TABLE I: The boundary conditions for thermodynamic functions.

	U	C	Y	S_E/k_B
$T \rightarrow 0$	0	0	0	0
$T \rightarrow \infty$	$ cN_U $	0	N_U	$\ln N_{state}$
$c \rightarrow 0$	0	0	N_U	$\ln N_{state}$
$c \rightarrow \infty$	0	0	0	0

the deviation of $P_{top}N_{state}$ from 1 measures how far the spin-fluctuation is away from the maximum value. Examples of P_g and $P_{top}N_{state}$ are shown in Fig. 2. To show the T -sensitivity, $U/k_B T$ and \mathfrak{C}/k_B are also plotted. It is found that T_1 is the position that P_g starts to decline from 1. Thus T_1 marks the temperature of the second condensation. T_2 is the place that $P_{top}N_{state}$ starts to decrease from 1. Thus T_2 marks the maxima of spin-fluctuation and entropy. To describe it quantitatively, T_1 and T_2 are defined at which $P_g = 0.95$ and $P_{top}N_{state} = 0.95$, respectively. When T is very low, P_g can be approximated by $P_{g,appr} = 1/(1 + e^{-\beta E_{gap,1}})$, and accordingly $T_1 = 0.34 E_{gap,1}/k_B$.

Furthermore, our calculation demonstrates that $U/k_B T$ is always less than $3/2$ as shown in Fig. 2. It implies that, disregarding N and interactions, the internal energy contributed from all the spin degrees of freedom is even smaller than the energy assigned to the spatial motion for a single particle. This fact manifests how small the energy is involved in the spin-space.

Let the energy of the lowest state with a spatial mode excited be E_1^{ex} , which can be obtained by solving the equation given in the ref.[19, 20] How weak the interference from the spatial mode would be depends on the gap $E_{gap2} = E_1^{ex} - E_{top}$. When the gap is sufficiently large, the probability of staying in the spatially excited levels is negligible. The temperature at which $e^{-\beta E_{gap,2}} = 0.05$ is defined as T_3 (i.e., $T_3 = \frac{E_{gap,2}}{3k_B}$). When $T < T_3$, the spin-space is decoupled from the spatial modes.

When both N and M are fixed, the dependence of T_1 , T_2 , and T_3 on ω is shown in Fig. 3. Note that a larger ω will lead to a more compact $\phi(\mathbf{r})$ (smaller in size) and thereby a stronger $|c|$. Hence, all the T_1, T_2 and T_3 will become higher when ω increases. For Rb, the second condensation can be realized at $T_1 = 10^{-9}K$ when $\omega = 10^{4.5}s^{-1}$ and $N = 1000$ (Fig.3a). If ω and/or N are larger, T_1 is even higher. For Na, $E_{gap1} \propto M'$, therefore T_1 depends on M seriously. When $M = N - 2$ and $N = 1000$, T_1 would be higher than $10^{-9}K$ if $\omega > 10^{3.7}s^{-1}$ (3c).

When N is small T_3 can be quite high (say, $T_3 > 10^{-8}K$ if $\omega > 10^4s^{-1}$ (3b,3d). It implies that a nearly pure spin-system can be created experimentally. When N is larger, due to the cross over of the highest member of the ground band and the lowest member of the excited band, T_3 does not exist unless M is close to N (3a and 3c). In 3a (3c) and when $\omega = 10^{3.1}s^{-1}(10^{2.28}s^{-1})$, a cross over of T_3 and T_2 occurs. When ω is smaller than the value, the domain (T_1, T_2) is under T_3 so that the whole process of the increase of entropy from zero to being maximized is free from the interference of the spatial modes.

Since the thermodynamic functions change greatly in the T -sensitive domain, the spin-texture and spin-component μ should be modulated accordingly. For ϑ_{SM}^N , the probability of a particle in μ can be calculated from

Eq. (10) in Ref. [21]. In particular, when $\mu = 0$ the probability is

$$P_0^{SM} = \frac{S(S+1)(2N+1) - M^2(2N+3) - N}{N(2S+3)(2S-1)} \quad (4)$$

When the thermo-fluctuation is taken into account, we define

$$\bar{P}_0^M(T) = \frac{1}{Z} \sum_S P_0^{SM} e^{-\beta E_S} \quad (5)$$

and the population of $\mu = 0$ component is $N\bar{P}_0^M(T)$. Examples of $\bar{P}_0^M(T)$ are given in Fig. 4. When $T \rightarrow 0$ and for Rb, $\bar{P}_0^M(0) = P_0^{NM} = \frac{N^2 - M^2}{N(2N-1)}$, while for Na, $\bar{P}_0^M(0) = P_0^{MM} = \frac{N-M}{N(2M+3)}$. In both cases, $\bar{P}_0^M(0)$ decreases with M . As T increases, $\bar{P}_0^M(T)$ remains unchanged until T enters into the T -sensitive domain. Thus the borders of the T -sensitive domain can be evaluated by measuring $\bar{P}_0^M(T)$.

When a magnetic field B is applied, the linear Zeeman term can be dropped for the M -conserved systems, the quadratic Zeeman term corresponds to $H_B = q \sum_i \mathbf{f}_{iz}^2$, where \mathbf{f}_{iz} is the z -component of the spin-operator for the i -th particle. Under H_B the states with different S will mix up, and the i -th eigenstates will appear as $\Psi_{i,M}^B = \sum_S C_S^{B,i} \Psi_{SM}$. The matrix elements $\langle \vartheta_{S'M}^N | H_B | \vartheta_{SM}^N \rangle$ are shown in Eqs. (3,4,6,7) of Ref. [21]. By diagonalizing the matrix of $H + H_B$, the eigenenergies E_i^B and $\Psi_{i,M}^B$ can be obtained. It is found that there is always a turning point B_0 so that the spectra will remain nearly unchanged when $B \leq B_0$ as shown in Fig. 5, where $B_0 = 0.5mG$. Based on the perturbation theory $\Psi_{i,M}^{B+\varepsilon}$ would be closer to $\Psi_{i,M}^B$ (where ε is a small quantity) if the levels in the neighborhood of E_i^B are wider separated. Accordingly, the B_0 for Rb is much larger than that for Na because the low-lying levels of the former are much splitting. Furthermore, a smaller N can lead to a larger $\int |\phi(\mathbf{r})|^4 d\mathbf{r}$, therefore a larger $|c|$ and accordingly a larger level-separation resulting also in a larger B_0 . For Na, the level-separation depends on \mathbf{M} , hence a larger M will also lead to a larger B_0 . Since all the thermodynamic properties depend solely on the spectra, the invariance of the spectra implies that all the features at $B = 0$ will remain unchanged when $B \leq B_0$.

In summary, the M -conserved pure spin-systems of cold Rb and Na atoms at $B = 0$ are studied, three domains of T are found. The effect of a residual B has been evaluated. The main results are:

1) $(0, T_1)$ is a T -insensitive domain originated from the gap $E_{gap,1}$, and $T_1 = 0.34 E_{gap,1}/k_B$ marks the *second condensation* [12]. It is reported (Fig. 2 of Ref. [12]) that, for a spin-3 condensation, M depends on T in general, but becomes insensitive to T when $T \rightarrow 0$ and B is sufficiently weak. Thus, the appearance of the

T -insensitive domain during $T \rightarrow 0$ might be a common phenomenon.

2) (T_1, T_2) is a T -sensitive domain, where the thermo-fluctuation keeps strengthening. $U \propto T$ and $S_E \propto \ln T$ roughly hold, and $U/k_B T < \frac{3}{2}$ holds. The location of this domain can be known by measuring $\bar{P}_0^M(T)$.

3) (T_2, T_3) is again a T -insensitive domain with $T_3 = \frac{E_{gap,2}}{3k_B}$. Due to the gap $E_{gap,2}$, the excitation of spatial modes is suppressed.

4) Both $E_{gap,1}$ and $E_{gap,2}$ can be tuned by changing ω , N , and M . Correspondingly, T_1 , T_2 , and T_3 also change. A larger N (for Rb) or a larger $|M|$ (for Na) will lead to a larger $E_{gap,1}$ and the second condensation can be realized at higher temperature. The domain (T_1, T_2) can be compressed by reducing E_{top} (i.e., by increasing M). In particular, the low-dimensional systems are notable for application. For example, a 2-level system can be formed by fixing $M = N - 2$.

5) The present techniques can provide a shield so that the effect of a residual B is negligible. On the other hand, when B is stronger, its effect should be studied further.

6) It is also possible to consider an optical-lattice (OL) potential, or maybe an HP-OL combination. In that case, a deep OL may additionally freeze the spatial mode to realize the pure spin-system.

As a final remarks, the two gaps $E_{gap,1}$ and $E_{gap,2}$ are in general crucial to the physics at $T < T_c$.

Acknowledgment: The project is supported by the National Basic Research Program of China (2008AA03A314, 2012CB821400), NSFC projects (11274393, 11074310, 11275279), RFDPE of China (20110171110026) and NCET-11-0547.

* Electronic address: stsbcg@mail.sysu.edu.cn

- [1] J. Stenger, et al., Nature 396, 345 (1998).
- [2] T. L. Ho, Phys. Rev. Lett. 81, 742 (1998).
- [3] T. Ohmi and K. Machida, J. Phys. Soc. Jpn. 67, 1822 (1998).
- [4] C. K. Law, H. Pu, and N. P. Bigelow, Phys. Rev. Lett. 81, 5257 (1998).
- [5] H. Pu, C. K. Law, S. Raghavan, J. H. Eberly, and N. P. Bigelow, Phys. Rev. A 60, 1463 (1999).
- [6] J. M. Zhang, S. Cui, H. Jing, D. L. Zhou, W. M. Liu, Phys. Rev. A 80, 043623(2009).
- [7] M. S. Chang, Q. Qin, W. X. Zhang, L. You, and M. S. Chapman, Nature Physics 1, 111 (2005).
- [8] See the recent review: Y. Kawaguchi and M. Ueda, Phys. Rep. 520, 253 (2012), and references therein.
- [9] H. Jing, D. S. Goldbaum, L. Buchmann, P. Meystre, Phys. Rev. Lett. 106, 223601(2011).

- [10] B. Pasquiou, E. Marechal, G. Bismut, P. Pedri, L. Vernac, O. Gorceix, and B. Laburthe-Tolra, Phys. Rev. Lett. 106, 255303 (2011).
- [11] A. de Paz, A. Chotia, E. Marechal, P. Pedri, L. Vernac, O. Gorceix, and B. Laburthe-Tolra, arXiv:1212.5469.
- [12] B. Pasquiou, E. Marechal, L. Vernac, O. Gorceix, and B. Laburthe-Tolra, Phys. Rev. Lett. 108, 045307 (2012).
- [13] A. D. O’Connell, et al., Nature (London) 464, 697 (2010).
- [14] M. Walter, B. Doran, D. Gross, M. Christandl, Science 340, 1205-1208 (2013).
- [15] H. K. Pechkis, J. P. Wrubel, A. Schwettmann, P. F. Griffin, R. Barnett, E. Tiesinga, and P. D. Lett, Phys. Rev. Lett. 111, 025301 (2013).
- [16] K. Yamada, Prog. Theor. Phys. 67, 443, (1982).
- [17] C.G. Bao and Z.B. Li, Phys. Rev. A 70, 043620 (2004).
- [18] J. Katriel, Mol. Struct.:THEOCHEM 547,1 (2001).
- [19] C.G. Bao and Z.B. Li, Phys. Rev. A 72, 043614 (2005).
- [20] W. Pang, Z.B. Li, and C.G. Bao, J. Phys. B: At.Mol.Opt.Phys. 40, 577 (2007).
- [21] C.G. Bao, J. Phys. A: Math. Theor. 45, 235002 (2012).

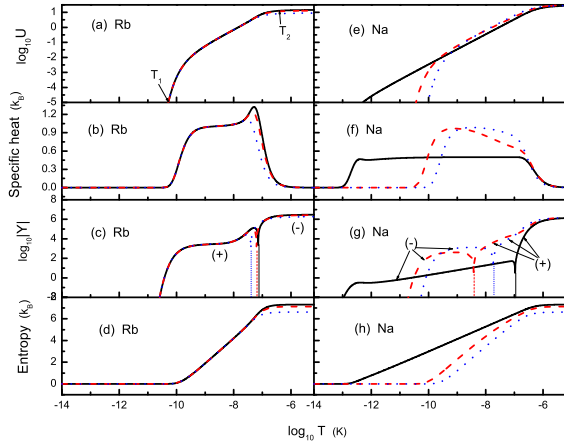


FIG. 1: (Color online). $\log U$, C , $\log|Y|$, and S_E of Rb (left column) and Na (right column) condensates versus $\log_{10} T$. The unit of U is $\hbar\omega$. $N = 3000$ and $\omega = 300 \times 2\pi$ are assumed. M is given at 0 (solid line), 500 (dash), and 1500 (dot). For (c) and (e), the sign of Y is marked by the curves.

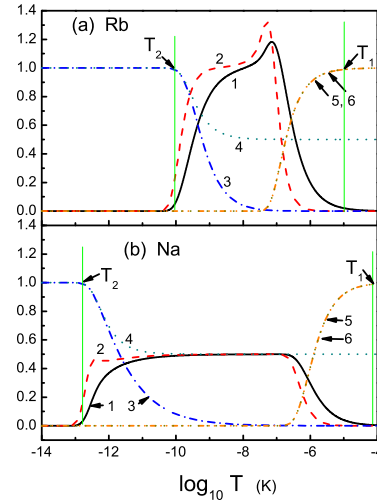


FIG. 2: (Color online). Six functions of Rb (a) and Na (b) versus $\log_{10} T$. Curve “1” is for $U/k_B T$, “2” is for C/k_B , “3” is for P_g , “4” is for $P_{g,appr}$, “5” is for $P_{top}N_{state}$, and “6” is for $P_{top,ap}N_{state}$. ($P_{top,ap}$ is obtained by transforming the summation involved into an integration). $N = 3000$, $M = 0$, and $\omega = 300 \times 2\pi$ are used.

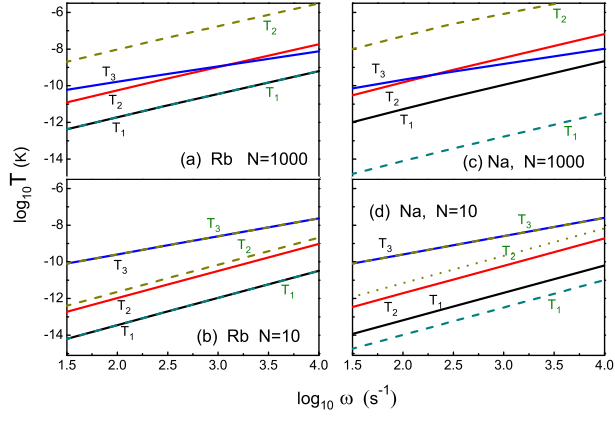


FIG. 3: (Color online). T_1, T_2 and T_3 versus ω . Solid lines are for $M = N - 2$, dash for $M = 0$. When $M = 0$ and $N = 1000$, T_3 does not exist.

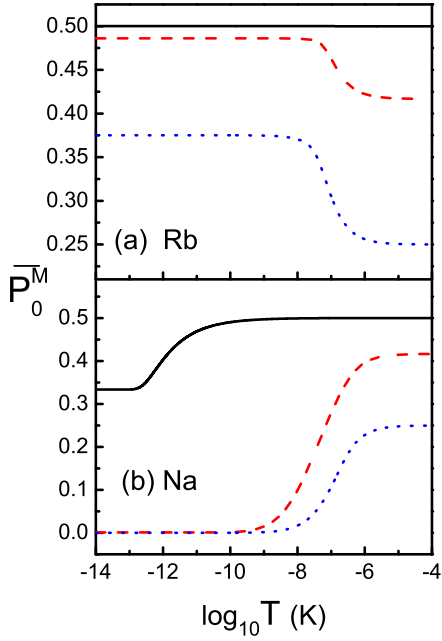


FIG. 4: (Color online). $\overline{P}_0^M(T)$ versus T for Rb (a) and Na (b). The parameters and the three choices of M are the same as in Fig. 1.

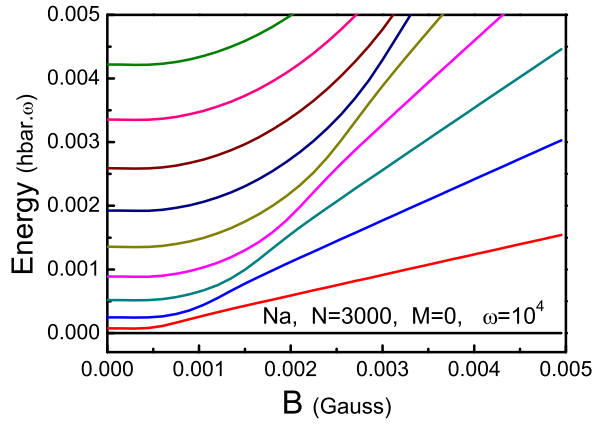


FIG. 5: (Color online). The spectrum of a Na condensate versus B . The lowest ten curves are plotted.